

Two-Dimensional Radiative Heat Transfer in a Planar Layer Bounded by Nonisothermal Walls

A. L. Crosbie* and J. W. Koewing†
University of Missouri-Rolla, Rolla, Mo.

The emissive power and radiative flux at the boundaries are calculated for a two-dimensional, finite, planar, gray, absorbing-emitting-scattering medium bounded by nonisothermal black walls. The medium is in radiative equilibrium and the scattering phase function is composed of a spike in the forward direction superimposed on an isotropic background. Exact radiative transfer theory is used to formulate the problem. Using the principle of superposition, the results for any step variation in the wall temperatures are expressed in terms of universal functions for the semi-infinite step variation in wall temperature. Thus, many different wall temperature distributions can be handled. The results are also directly applicable to a nongray medium with spectral windows.

Nomenclature

$\mathcal{E}_n(\tau, \beta)$	= generalized exponential integral
$E_n(\tau)$	= exponential integral
$E_n(\eta, \tau)$	= two-dimensional attenuation functions
f	= fraction of radiation scattered in the forward direction
$F_\beta(\tau, \tau_0)$	= dimensionless z component of the radiative flux for cosine-varying case
$F(\tau_y, \tau_z; \tau_0)$	= dimensionless z component of the radiative flux for semi-infinite step case
$g(\beta)$	= Fourier transform for wall temperature
I	= radiant intensity
$K_0(t)$	= modified Bessel function of order one
L	= thickness of the medium
$P(\cos\Theta)$	= scattering phase function
\bar{q}	= radiative flux
q_z	= z component of the radiative flux
$R_\beta(\mu, \mu')$	= generalized reflection function
S	= source function
$T_\beta(\mu, \mu')$	= generalized transmission function
T	= temperature
X_β, Y_β	= generalized X and Y functions
$\alpha(\nu)$	= spectral distribution of the absorption and scattering coefficients
β	= spatial frequency of incident radiation
β_e	= extinction coefficient ($\kappa + \sigma_s$)
$\delta(\mu)$	= Dirac delta function
Θ	= angle between incident and scattered intensity
κ	= absorption coefficient
μ	= cosine of the polar angle
ν	= frequency
σ	= Stefan-Boltzmann constant
σ_s	= scattering coefficient
τ_0	= optical thickness, $(\beta_e - f\sigma_s)L$
τ_s	= optical distance, $(\beta_e - f\sigma_s)s$
τ_y, τ_z	= optical coordinates, $(\beta_e - f\sigma_s)y, (\beta_e - f\sigma_s)z$
$\phi_\beta(\tau, \tau_0)$	= dimensionless emissive power for the cosine-varying case
ϕ	= azimuthal angle
$\phi(\tau_y, \tau_z; \tau_0)$	= dimensionless emissive power for the semi-infinite case

$\psi(x, \beta)$	$= (\frac{1}{2})[1 + \beta^2(1 - x^2)]^{-1/2}$
$\psi_1(x, \beta)$	$= (1 + \beta^2)/[1 + \beta^2(1 - x^2)]^{3/2}$
Ω	= solid angle

Introduction

HISTORICALLY, radiative heat transfer in a scattering medium has been analyzed with a one-dimensional model. The one-dimensional model considerably reduces the mathematical complexity. However, many physical situations cannot be characterized by a one-dimensional model, and a multidimensional analysis is necessary. Much work needs to be done in the area of multidimensional scattering.

A recent review of multidimensional radiative transfer in a scattering medium by Crosbie and Linsenbardt¹ reveals a very limited number of investigations which considered emission in addition to scattering. Bobco² and Love and Turner^{3,4} considered an isothermal semi-infinite slab, while Love and Stockham⁵ analyzed an isothermal finite cylinder. The time-consuming Monte Carlo technique was used by Love and associates, while Bobco used an approximate approach. All of these studies considered isotropic scattering. Only the investigation of Love and Stockham⁵ included anisotropic scattering. A nonisothermal medium was not considered in any of the previous investigations.

In a related series of articles,⁶⁻¹⁰ Breig and Crosbie studied two-dimensional radiative equilibrium in an absorbing-emitting planar medium exposed to spatially varying radiation. The problem was formulated⁶ using exact radiative transfer theory, and numerical results were presented for the semi-infinite^{7,8} and finite^{9,10} medium. The results for the finite medium were limited to the cosine-varying boundary condition.

The primary objective of the present investigation is to obtain exact numerical results for a gray, absorbing-emitting-scattering planar medium bounded by nonisothermal black walls. Specifically, the emissive power and radiative flux at the boundaries are calculated when the wall temperature is presented by a series of steps. While this situation is somewhat ideal, the results represent "benchmark" solutions. For more complex physical situations, approximate procedures for handling the radiative transfer are necessary because of computer time limitations. In order to evaluate these procedures, it is extremely helpful to have exact test cases available.² Also, the results presented should be useful in analyzing other boundary conditions.

Physical Model

The coordinate system and geometry are illustrated in Fig. 1. The present investigation is based on the following assumption.

Received Feb. 15, 1978; revision received Aug. 28, 1978. Copyright © American Institute of Aeronautics and Astronautics, Inc., 1978. All rights reserved.

Index category: Radiation and Radiative Heat Transfer.

*Professor, Thermal Radiative Transfer Group, Dept. of Mechanical and Aerospace Engineering, Member AIAA.

†Graduate Student; presently with Westinghouse Electric Corp., West Mifflin, Pa.

tions: 1) two-dimensional transfer, 2) steady-state temperature and intensity, 3) absorbing-emitting-scattering medium, 4) gray medium, 5) local thermodynamic equilibrium, 6) no conduction or convection (radiative equilibrium), 7) refractive index of unity, and 8) black walls. Under these assumptions, the transport equation for the radiant intensity I can be expressed as

$$\frac{dI}{ds} + \beta_e I = \mu \frac{\partial I}{\partial z} + \sqrt{1-\mu^2} \sin\phi \frac{\partial I}{\partial y} + \beta_e I = \frac{\kappa \sigma T^4}{\pi} + \frac{\sigma_s}{4\pi} \int_0^{2\pi} \int_{-1}^{+1} I P(\cos\Theta) d\mu' d\phi' \quad (1)$$

Θ is the angle between the incident (μ', ϕ') and scattered intensity (μ, ϕ) .

The phase function is approximated by a spike in the forward direction superimposed on an isotropic background, i.e.,

$$P(\cos\Theta) = 4\pi f \delta(\mu - \mu') \delta(\phi - \phi') + (1-f) \quad (2)$$

where δ is the Dirac delta function and f is the fraction of the radiation scattered in the forward direction. The quantity f is also equal to the asymmetry factor $\int_{4\pi} P(\cos\Theta) \cos\Theta (d\Omega/4\pi)$. The utility of this phase function has been discussed by Joseph, Wiscombe, and Weinman.¹¹ The strong forward component is characteristic of the scattering phase function for large particles. Thus, the transport equation becomes

$$\frac{dI}{ds} + (\beta_e - f\sigma_s) I = \frac{\kappa \sigma T^4}{\pi} + \sigma_s (1-f) S \quad (3)$$

where the source function is defined

$$S = \frac{1}{4\pi} \int_{4\pi} I d\Omega = \frac{1}{4\pi} \int_0^{2\pi} \int_{-1}^{+1} I d\mu' d\phi' \quad (4)$$

The conservation of energy for the radiative equilibrium is:

$$\vec{\nabla} \cdot \vec{q} = \int_{4\pi} \frac{dI}{ds} d\Omega = 4\pi \kappa \left[\frac{\sigma T^4}{\pi} - S \right] = 0 \quad (5)$$

Therefore,

$$S = \sigma T^4 / \pi \quad (6)$$

and the transport equation becomes

$$\frac{dI}{d\tau_s} + I = \frac{\sigma T^4}{\pi} \quad (7)$$

where $\tau_s = (\beta_e - f\sigma_s)s$. Inspection of this equation reveals that it is identical to the transport equation for a nonscattering

medium with an effective absorption coefficient $(\beta_e - f\sigma_s)$. Thus, isotropic scattering ($f=0$) increases the effective absorption coefficient, while anisotropic scattering in the forward direction reduces it. In terms of optical coordinates $[\tau_z = (\beta_e - f\sigma_s)z, \tau_y = (\beta_e - f\sigma_s)y]$, the transport equation is given by

$$\mu \frac{\partial I}{\partial \tau_z} + \sqrt{1-\mu^2} \sin\phi \frac{\partial I}{\partial \tau_y} + I = \frac{\sigma T^4}{\pi} \quad (8)$$

Following the procedure of Breig and Crosbie,⁷ the energy equation and the z component of the radiative flux can be expressed as

$$\begin{aligned} \sigma T^4(\tau_y, \tau_z) &= \int_{-\infty}^{\infty} \sigma T_1^4(\tau_y') E_2(\tau_y - \tau_y', \tau_z) d\tau_y' \\ &+ \int_{-\infty}^{\infty} \sigma T_2^4(\tau_y') E_2(\tau_y - \tau_y', \tau_0 - \tau_z) d\tau_y' \\ &+ \int_{-\infty}^{\infty} \int_0^{\tau_0} \sigma T^4(\tau_y', \tau_z') E_1(\tau_y - \tau_y', \tau_z - \tau_z') d\tau_z' d\tau_y' \end{aligned} \quad (9)$$

$$\begin{aligned} q_z(\tau_y, \tau_z) &= \int_{-\infty}^{\infty} \sigma T_1^4(\tau_y') E_3(\tau_y - \tau_y', \tau_z) d\tau_y' \\ &- \int_{-\infty}^{\infty} \sigma T_2^4(\tau_y') E_3(\tau_y - \tau_y', \tau_0 - \tau_z) d\tau_y' \\ &+ \int_{-\infty}^{\infty} \int_0^{\tau_0} \sigma T^4(\tau_y', \tau_z') E_2(\tau_y - \tau_y', \tau_z - \tau_z') d\tau_z' d\tau_y' \end{aligned} \quad (10)$$

where

$$E_1(\eta, \tau) = \frac{1}{2\pi} \int_0^{\tau} K_0(t\sqrt{\eta^2 + \tau^2}) dt \quad (11a)$$

$$E_2(\eta, \tau) = \frac{\tau}{2\pi} \int_0^{\tau} \int_0^{\tau} K_0(xy\sqrt{\eta^2 + \tau^2}) x dy dx \quad (11b)$$

$$E_3(\eta, \tau) = \frac{\tau^2}{\pi} \int_0^{\tau} \int_0^{\tau} \int_0^{\tau} K_0(xyz\sqrt{\eta^2 + \tau^2}) xy^2 dx dy dz \quad (11c)$$

and $K_0(t)$ is the modified Bessel function of order one. The energy equation, Eq. (9), is linear in the emissive power σT^4 but is complicated by its two-dimensional character. The problem can be simplified by representing the emissive powers at the wall by a Fourier integral, i.e.,

$$\sigma T_1^4(\tau_y) = \int_{-\infty}^{\infty} g_1(\beta) \exp(i\beta\tau_y) d\beta \quad (12a)$$

$$\sigma T_2^4(\tau_y) = \int_{-\infty}^{\infty} g_2(\beta) \exp(i\beta\tau_y) d\beta \quad (12b)$$

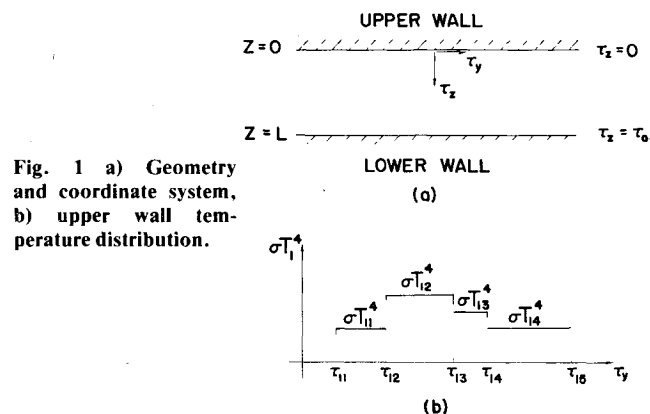
where $g_1(\beta)$ and $g_2(\beta)$ are given by

$$g_1(\beta) = \frac{1}{2\pi} \int_{-\infty}^{\infty} \sigma T_1^4(\tau_y) \exp(-i\beta\tau_y) d\tau_y \quad (13a)$$

$$g_2(\beta) = \frac{1}{2\pi} \int_{-\infty}^{\infty} \sigma T_2^4(\tau_y) \exp(-i\beta\tau_y) d\tau_y \quad (13b)$$

Utilization of Eqs. (12) and the principle of superposition enables Eqs. (9) and (10) to be written as

$$\begin{aligned} \sigma T^4(\tau_y, \tau_z) &= \int_{-\infty}^{\infty} g_1(\beta) \exp(i\beta\tau_y) \phi_{\beta}(\tau_z; \tau_0) d\beta \\ &+ \int_{-\infty}^{\infty} g_2(\beta) \exp(i\beta\tau_y) \phi_{\beta}(\tau_0 - \tau_z; \tau_0) d\beta \end{aligned} \quad (14)$$



$$q_z(\tau_y, \tau_z) = \int_{-\infty}^{\infty} g_1(\beta) \exp(i\beta\tau_y) F_\beta(\tau_z; \tau_0) d\beta \\ - \int_{-\infty}^{\infty} g_2(\beta) \exp(i\beta\tau_y) F_\beta(\tau_0 - \tau_z; \tau_0) d\beta \quad (15)$$

where

$$\phi_\beta(\tau_z; \tau_0) = \frac{1}{2} \mathcal{E}_2(\tau_z, \beta) \\ + \frac{1}{2} \int_0^{\tau_0} \phi_\beta(\tau'_z; \tau_0) \mathcal{E}_1(|\tau_z - \tau'_z|, \beta) d\tau'_z \quad (16)$$

$$F_\beta(\tau_z; \tau_0) = 2\mathcal{E}_3(\tau_z, \beta) \\ + 2 \int_0^{\tau_0} \phi_\beta(\tau'_z; \tau_0) \operatorname{sgn}(\tau_z - \tau'_z) \mathcal{E}_2(|\tau_z - \tau'_z|, \beta) d\tau'_z \quad (17)$$

The generalized exponential integrals are defined as¹²

$$\mathcal{E}_1(\tau, \beta) = \int_0^\infty \exp(-\tau\sqrt{t^2 + \beta^2}) \frac{dt}{\sqrt{t^2 + \beta^2}} \quad (18a)$$

$$\mathcal{E}_2(\tau, \beta) = \int_0^\infty \exp(-\tau\sqrt{t^2 + \beta^2}) \frac{dt}{t^2} \quad (18b)$$

$$\mathcal{E}_3(\tau, \beta) = \tau \int_0^\infty \mathcal{E}_2(\tau t, \beta/t) dt \quad (18c)$$

Thus, if the universal functions ϕ_β and F_β are known, any temperature-distribution can be handled with Eqs. (14) and (15). Physically, the functions ϕ_β and F_β represent the emissive power and radiative flux for the medium subjected to cosine varying diffuse radiation, i.e., $\sigma T_1^4(\tau_y) = \cos(\beta\tau_y)$ and $\sigma T_2^4(\tau_y) = 0$. β represents the spatial frequency of the incident radiation. When β is zero, the incident radiation is uniform, the generalized exponential integrals reduce to the exponential integrals [$\mathcal{E}_n(\tau, 0) = E_n(\tau)$], and the problem reduces to the standard one-dimensional case, i.e.,

$$\phi_{\beta=0}(\tau_z; \tau_0) = \frac{1}{2} E_2(\tau_z) \\ + \frac{1}{2} \int_0^{\tau_0} \phi_{\beta=0}(\tau'_z; \tau_0) E_1(|\tau_z - \tau'_z|) d\tau'_z \quad (19)$$

$$F_{\beta=0}(\tau_z; \tau_0) = 2E_3(\tau_z) \\ + 2 \int_0^{\tau_0} \phi_{\beta=0}(\tau'_z; \tau_0) \operatorname{sgn}(\tau_z - \tau'_z) E_2(|\tau_z - \tau'_z|) d\tau'_z \quad (20)$$

Instead of evaluating Eqs. (14) and (15) for a large number of different boundary conditions, a simple but physically realistic boundary condition is considered. The wall temperatures are approximated by a finite number of steps, i.e.,

$$\sigma T_1^4(\tau_y) = \frac{1}{2} \sum_{k=1}^M \sigma T_{1k}^4 [\operatorname{sgn}(\tau_y - \tau_{1k}) - \operatorname{sgn}(\tau_y - \tau_{1k+1})] \quad (21a)$$

$$\sigma T_2^4(\tau_y) = \frac{1}{2} \sum_{k=1}^N \sigma T_{2k}^4 [\operatorname{sgn}(\tau_y - \tau_{2k}) - \operatorname{sgn}(\tau_y - \tau_{2k+1})] \quad (21b)$$

Noting that

$$\operatorname{sgn}(\tau - \tau_k) = \frac{1}{\pi} \int_{-\infty}^{\infty} \sin[\beta(\tau - \tau_k)] \frac{d\beta}{\beta} \\ = -\frac{1}{\pi} \int_{-\infty}^{\infty} i \exp[i\beta(\tau - \tau_k)] \frac{d\beta}{\beta} \quad (22)$$

the g functions are:

$$g_1(\beta) = \frac{i}{2\pi\beta} \sum_{k=1}^M \sigma T_{1k}^4 [-\exp(-i\beta\tau_{1k}) + \exp(-i\beta\tau_{1k+1})] \quad (23a)$$

$$g_2(\beta) = \frac{i}{2\pi\beta} \sum_{k=1}^N \sigma T_{2k}^4 [-\exp(-i\beta\tau_{2k}) + \exp(-i\beta\tau_{2k+1})] \quad (23b)$$

Substitution of these equations into Eqs. (14) and (15) yields

$$\sigma T^4(\tau_y, \tau_z) \\ = \sum_{k=1}^M \sigma T_{1k}^4 [\phi(\tau_y - \tau_{1k}, \tau_z; \tau_0) - \phi(\tau_y - \tau_{1k+1}, \tau_z; \tau_0)] \\ + \sum_{k=1}^N \sigma T_{2k}^4 [\phi(\tau_y - \tau_{2k}, \tau_0 - \tau_z; \tau_0) - \phi(\tau_y - \tau_{2k+1}, \tau_0 - \tau_z; \tau_0)] \quad (24)$$

$$q_z(\tau_y, \tau_z) = \\ \sum_{k=1}^M \sigma T_{1k}^4 [F(\tau_y - \tau_{1k}, \tau_z; \tau_0) - F(\tau_y - \tau_{1k+1}, \tau_z; \tau_0)] \\ - \sum_{k=1}^N \sigma T_{2k}^4 [F(\tau_y - \tau_{2k}, \tau_0 - \tau_z; \tau_0) - F(\tau_y - \tau_{2k+1}, \tau_0 - \tau_z; \tau_0)] \quad (25)$$

where

$$\phi(\tau_y, \tau_z; \tau_0) = \frac{1}{\pi} \int_0^\infty \phi_\beta(\tau_z; \tau_0) \sin(\beta\tau_y) \frac{d\beta}{\beta} \quad (26)$$

$$F(\tau_y, \tau_z; \tau_0) = \frac{1}{\pi} \int_0^\infty F_\beta(\tau_z; \tau_0) \sin(\beta\tau_y) \frac{d\beta}{\beta} \quad (27)$$

Physically, the functions ϕ and F represent the emissive power and radiative flux for a medium subjected to a semi-infinite step of diffuse radiation, i.e., $\sigma T_1^4(\tau_y) = \frac{1}{2} \operatorname{sgn}(\tau_y)$ and $\sigma T_2^4(\tau_y) = 0$. In the preceding relations, the following identities are useful:

$$\phi(-\tau_y, \tau_z; \tau_0) = -\phi(\tau_y, \tau_z; \tau_0) \quad (28a)$$

$$F(-\tau_y, \tau_z; \tau_0) = -F(\tau_y, \tau_z; \tau_0) \quad (28b)$$

$$\phi(\infty, \tau_z; \tau_0) = \frac{1}{2} \phi_{\beta=0}(\tau_z; \tau_0) \quad (28c)$$

$$F(\infty, \tau_z; \tau_0) = \frac{1}{2} F_{\beta=0}(\tau_z; \tau_0) \quad (28d)$$

By evaluating the functions ϕ and F , a wide range of problems can be solved.

For example, the case considered by Taitel,¹³ i.e.,

$$\sigma T_1^4 = \begin{cases} \sigma T_{11}^4 & \tau_y < 0 \\ \sigma T_{12}^4 & \tau_y > 0 \end{cases} \quad \sigma T_2^4 = \begin{cases} \sigma T_{21}^4 & \tau_y < 0 \\ \sigma T_{22}^4 & \tau_y > 0 \end{cases} \quad (29)$$

can be expressed in terms of the present investigation as follows: $M=N=2$, $\tau_{11}=\tau_{21}=-\infty$, $\tau_{12}=\tau_{22}=0$, and $\tau_{13}=\tau_{23}=\infty$. Thus, the emissive power and radiative flux are:

$$\sigma T^4(\tau_y, \tau_z) = \frac{1}{2} (\sigma T_{11}^4 + \sigma T_{12}^4) \phi_{\beta=0}(\tau_z; \tau_0) \\ + (\sigma T_{12}^4 - \sigma T_{11}^4) \phi(\tau_y, \tau_z; \tau_0) + \frac{1}{2} (\sigma T_{21}^4 + \sigma T_{22}^4) \\ \times \phi_{\beta=0}(\tau_0 - \tau_z; \tau_0) + (\sigma T_{22}^4 - \sigma T_{21}^4) \phi(\tau_y, \tau_0 - \tau_z; \tau_0) \quad (30)$$

$$q_z(\tau_y, \tau_z) = \frac{1}{2}(\sigma T_{11}^4 + \sigma T_{12}^4)F_{\beta=0}(\tau_z, \tau_0) + (\sigma T_{12}^4 - \sigma T_{11}^4) \\ \times F(\tau_y, \tau_z; \tau_0) - \frac{1}{2}(\sigma T_{21}^4 + \sigma T_{22}^4)F_{\beta=0}(\tau_0 - \tau_z; \tau_0) \\ - (\sigma T_{22}^4 - \sigma T_{21}^4)F(\tau_y, \tau_0 - \tau_z; \tau_0) \quad (31)$$

These expressions can be further simplified by taking into account the one-dimensional identities, i.e.,

$$\phi_{\beta=0}(\tau_z; \tau_0) + \phi_{\beta=0}(\tau_0 - \tau_z; \tau_0) = I \quad (32a)$$

$$F_{\beta=0}(\tau_z; \tau_0) = F_{\beta=0}(\tau_0 - \tau_z; \tau_0) \quad (32b)$$

Thus, it is not necessary to calculate the results for each set of temperatures, T_{11} , T_{12} , T_{21} , and T_{22} , if the functions ϕ and F are known. If both walls have the same distribution, i.e., $T_{11} = T_{21}$ and $T_{12} = T_{22}$, the emissive power and radiative flux become

$$\sigma T^4(\tau_y, \tau_z) = \frac{1}{2}(\sigma T_{11}^4 + \sigma T_{22}^4) + (\sigma T_{22}^4 - \sigma T_{11}^4) \\ \times [\phi(\tau_y, \tau_z; \tau_0) + \phi(\tau_y, \tau_0 - \tau_z; \tau_0)] \quad (33)$$

$$q_z(\tau_y, \tau_z) = (\sigma T_{22}^4 - \sigma T_{11}^4) \\ \times [F(\tau_y, \tau_z; \tau_0) - F(\tau_y, \tau_0 - \tau_z; \tau_0)] \quad (34)$$

For this special case, it can be easily shown that

$$\sigma T^4(\tau_y, \tau_z) = \sigma T^4(\tau_y, \tau_0 - \tau_z) \quad (35a)$$

$$\sigma T^4(\tau_y, \tau_z) + \sigma T^4(-\tau_y, \tau_z) = \sigma T_{11}^4 + \sigma T_{22}^4 \quad (35b)$$

$$q_z(\tau_y, \tau_z) = -q_z(\tau_y, \tau_0 - \tau_z) = -q_z(-\tau_y, \tau_z) \quad (35c)$$

At large optical distances away from the origin $|\tau_y| \gg 1$, the temperature is constant and the radiative flux is zero. A one-dimensional analysis would predict $q_z = 0$ everywhere, while the two-dimensional analysis yields nonzero values near the origin.

Numerical Procedure

A procedure for calculating ϕ_β and F_β at the boundaries was developed by Breig and Crosbie.^{9,10} However, results were limited to only a few β values because of numerical difficulties. Far too few results were obtained to be able to evaluate integrals, Eqs. (26) and (27). As β became large ($\beta > 1$), the step size $\Delta\tau_0$ used in the numerical solution decreased rapidly, and it was impractical to obtain results for even moderate optical thicknesses because of excessive computational times. In addition, for large β , the numerical integration used to evaluate F_β became inaccurate.

With these difficulties in mind, the numerical procedure is modified. Using Ambarzumian's approach^{9,10} the equations for ϕ_β and F_β at the boundaries are:

$$\phi_\beta(0; \tau_0) = \frac{1}{2} \int_0^I \psi_I(x, \beta) X_\beta(x; \tau_0) dx \quad (36)$$

$$\phi_\beta(\tau_0; \tau_0) = \frac{1}{2} \int_0^I \psi_I(x, \beta) Y_\beta(x; \tau_0) dx \quad (37)$$

$$F_\beta(0; \tau_0) = I - \int_0^I \psi_I(x, \beta) \bar{Q}_\beta(0, x; \tau_0) dx \quad (38)$$

$$F_\beta(\tau_0; \tau_0) = 2\mathcal{E}_3(\tau_0, \beta) + \int_0^I \psi_I(x, \beta) \bar{Q}_\beta(\tau_0, x; \tau_0) dx \quad (39)$$

with

$$\bar{Q}_\beta(0, \mu; \tau_0) = \mu \int_0^I x' \psi_I(x', \beta) R_\beta(\mu, x') dx' / \sqrt{I + \beta^2} \quad (40)$$

$$\bar{Q}_\beta(\tau_0, \mu; \tau_0) = \mu \int_0^I x' \psi_I(x', \beta) T_\beta(\mu, x') dx' / \sqrt{I + \beta^2} \quad (41)$$

$$\psi_I(x, \beta) = (I + \beta^2) / [I + \beta^2(I - x^2)]^{3/2} \quad (42)$$

where R_β and T_β represent a generalized reflection and transmission functions, i.e.,

$$R_\beta(\mu, \mu') = [X_\beta(\mu; \tau_0) X_\beta(\mu'; \tau_0) \\ - Y_\beta(\mu; \tau_0) Y_\beta(\mu'; \tau_0)] / (\mu + \mu') \quad (43)$$

$$T_\beta(\mu, \mu') = [X_\beta(\mu'; \tau_0) Y_\beta(\mu; \tau_0) \\ - X_\beta(\mu; \tau_0) Y_\beta(\mu'; \tau_0)] / (\mu - \mu') \quad (44)$$

and X_β and Y_β represent generalized X and Y functions. Obviously, the generalized X and Y functions are key to all calculations and are evaluated from the following two coupled integro-differential equations:

$$X'_\beta(\mu; \tau_0) = \sqrt{I + \beta^2} Y_\beta(\mu; \tau_0) \int_0^I \psi(x, \beta) Y_\beta(x; \tau_0) (dx/x) \quad (45)$$

$$Y'_\beta(\mu; \tau_0) = -\sqrt{I + \beta^2} Y_\beta(\mu; \tau_0) / \mu \\ + \sqrt{I + \beta^2} X_\beta(\mu; \tau_0) \int_0^I \psi(x, \beta) Y_\beta(x; \tau_0) (dx/x) \quad (46)$$

where the prime indicates the derivative with respect to τ_0 and $\psi(x, \beta) = (1/2)[1 + \beta^2(1 - x^2)]^{-1/2}$. The initial conditions are simply $X_\beta(\mu; 0) = Y_\beta(\mu; 0) = 1$. Equations (45) and (46) are reduced to a system of $2\bar{N}$ ordinary differential equations by dividing the integral into two parts— $(0, \epsilon)$ and $(\epsilon, 1)$ —and approximating each subintegral by a Gaussian quadrature of order n ($\bar{N} = 2n$). Instead of the fourth-order Runge-Kutta method used by Breig and Crosbie⁹ with $n = 8$ and $\epsilon = 0.9$, this system of equations is solved by a fifth-order Runge-Kutta method developed by Butcher¹⁴ with $n = 15$, $\epsilon = 0.9$ for $\beta \leq 8$, and $\epsilon = 0.95$ for $\beta > 8$. This is done to insure accuracy, especially at small τ_0 . As the spatial frequency is increased, the step size is reduced (see Table 1).

When β is small, the integrals in Eqs. (36-38), (40), and (41) are evaluated with the same Gaussian quadrature ($\bar{N} = 30$) which is used in solving for the generalized X and Y functions. In order to avoid a singularity in Eq. (41) when $\mu = x$, a different order quadrature ($\bar{M} = 28$) is necessary to evaluate Eq. (39). The generalized X and Y functions at these additional quadrature points are calculated from differential Eqs. (45) and (46). These additional differential equations bring the total to $2(\bar{N} + \bar{M}) = 118$.

When β is large, the integrals containing ψ_I and $x\psi_I$ cannot be integrated accurately in the preceding forms. The function at $x = 1$ is subtracted off because most of the area under the integral is near $x = 1$, i.e.,

$$2\phi_\beta(0; \tau_0) = X_\beta(I; \tau_0) \\ + \int_0^I \psi_I(x, \beta) [X_\beta(x; \tau_0) - X_\beta(I; \tau_0)] dx \quad (47)$$

$$2\phi_\beta(\tau_0; \tau_0) = Y_\beta(I; \tau_0) \\ + \int_0^I \psi_I(x, \beta) [Y_\beta(x; \tau_0) - Y_\beta(I; \tau_0)] dx \quad (48)$$

$$F_\beta(0; \tau_0) = I - \bar{Q}_\beta(0, I + \Delta; \tau_0) \\ - \int_0^I \psi_I(x, \beta) [\bar{Q}_\beta(0, x; \tau_0) - \bar{Q}_\beta(0, I + \Delta; \tau_0)] dx \quad (49)$$

Table 1 Step sizes $\Delta\tau_0$ used to solve the differential equations for the X and Y functions

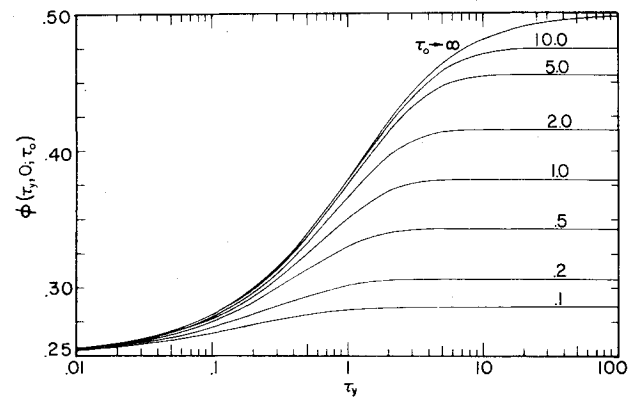
β ranges	$\Delta\tau_0$	
	$0 \leq \tau_0 \leq 0.01$	$\tau_0 > 0.01$
0 to 2.5	0.001	0.005
3 to 6	0.0005	0.0025
7 to 8	0.00025	0.00125
9 to 40	0.000125	0.000625
60 to 150	0.00005	0.0001
175 to 200	0.000025	0.00005
250 to 600	0.0000125	0.000025
800 to 1000	0.00000625	0.0000125
2000 to 5000	0.000003125	0.00000625
6000 to 10000	0.0000015625	0.000003125

Table 2 Cosine varying results for $\tau_0 = 0.10$

β	$\phi_\beta(0; \tau_0)$	$\phi_\beta(\tau_0; \tau_0)$	$F_\beta(0; \tau_0)$	$F_\beta(\tau_0; \tau_0)$
0.0	0.571017	0.428982	0.915702	0.915704
0.001	0.571017	0.428982	0.915702	0.915704
0.002	0.571017	0.428982	0.915702	0.915704
0.004	0.571017	0.428982	0.915702	0.915704
0.008	0.571017	0.428981	0.915702	0.915703
0.010	0.571017	0.428981	0.915702	0.915703
0.020	0.571014	0.428975	0.915703	0.915700
0.030	0.571010	0.428966	0.915705	0.915694
0.040	0.571005	0.428953	0.915707	0.915687
0.050	0.570997	0.428936	0.915710	0.915677
0.060	0.570989	0.428915	0.915714	0.915666
0.080	0.570966	0.428863	0.915723	0.915636
0.100	0.570938	0.428796	0.915735	0.915598
0.200	0.570702	0.428243	0.915835	0.915282
0.300	0.570319	0.427332	0.915988	0.914760
0.400	0.569806	0.426106	0.916220	0.914038
0.500	0.569180	0.424575	0.916496	0.913124
0.600	0.568461	0.422778	0.916819	0.912026
0.800	0.566818	0.418510	0.917587	0.909316
1.000	0.565006	0.413539	0.918481	0.905981
1.250	0.562647	0.406629	0.919720	0.901035
1.500	0.560291	0.399205	0.921046	0.895332
1.750	0.558001	0.391461	0.922429	0.888668
2.000	0.555809	0.383533	0.923838	0.882025
2.500	0.551761	0.367473	0.926676	0.866673
3.000	0.548155	0.351487	0.929477	0.849735
3.500	0.544950	0.335816	0.932199	0.831572
4.000	0.542094	0.320547	0.934821	0.812469
4.500	0.539538	0.305471	0.937332	0.792664
5.000	0.537241	0.291700	0.939728	0.772352
6.000	0.533286	0.265040	0.944180	0.730831
7.000	0.530012	0.240598	0.948199	0.688928
8.000	0.527263	0.218274	0.951819	0.647372
9.000	0.524929	0.197932	0.955079	0.606682
10.000	0.522927	0.179474	0.958017	0.567228
12.500	0.519000	0.140234	0.964174	0.475463
15.000	0.516143	0.109498	0.968785	0.394795
17.500	0.513691	0.085447	0.972795	0.325439
20.000	0.511322	0.066651	0.975853	0.266725
25.000	0.509970	0.040522	0.980392	0.176798
30.000	0.508288	0.024619	0.983557	0.115542
35.000	0.507112	0.014951	0.985861	0.074902
40.000	0.506227	0.009077	0.987607	0.048149
60.000	0.504155	1.2315E-03	0.991712	7.8206E-03
80.000	0.503117	1.6689E-04	0.993776	1.2100E-03
100.000	0.502494	2.2605E-05	0.995017	1.8201E-04
125.000	0.501995	1.8568E-06	0.996011	1.6629E-05
150.000	0.501662	1.5250E-07	0.996674	1.4910E-06
175.000	0.501424	1.2522E-08	0.997148	1.3194E-07
200.000	0.501246		0.997504	
250.000	0.500997		0.998003	
300.000	0.500830		0.998335	
400.000	0.500623		0.998751	
500.000	0.500498		0.999001	
600.000	0.500415		0.999167	
800.000	0.500311		0.999375	
1000.000	0.500249		0.999500	
1500.000	0.500166		0.999667	
2000.000	0.500124		0.999750	
3000.000	0.500083		0.999833	
4000.000	0.500062		0.999875	
5000.000	0.500050		0.999900	
8000.000	0.500031		0.999937	
10000.000	0.500025		0.999950	

Table 3 Cosine varying results for $\tau_0 = 0.5$

β	$\phi_\beta(0; \tau_0)$	$\phi_\beta(\tau_0; \tau_0)$	$F_\beta(0; \tau_0)$	$F_\beta(\tau_0; \tau_0)$
0.0	0.687332	0.312668	0.704169	0.704169
0.001	0.687335	0.312668	0.704169	0.704169
0.002	0.687332	0.312668	0.704169	0.704169
0.004	0.687331	0.312667	0.704170	0.704167
0.008	0.687323	0.312663	0.704173	0.704162
0.010	0.687326	0.312660	0.704175	0.704158
0.020	0.687310	0.312634	0.704194	0.704125
0.030	0.687282	0.312591	0.704226	0.704069
0.040	0.687243	0.312532	0.704269	0.703991
0.050	0.687194	0.312455	0.704326	0.703891
0.060	0.687133	0.312361	0.704395	0.703769
0.080	0.686979	0.312123	0.704570	0.703459
0.100	0.686781	0.311818	0.704794	0.703061
0.200	0.685161	0.309308	0.706640	0.699774
0.300	0.682554	0.305256	0.709618	0.694420
0.400	0.679125	0.299838	0.713598	0.687166
0.500	0.675007	0.293265	0.718424	0.678217
0.600	0.670374	0.285760	0.723928	0.667797
0.800	0.663176	0.268802	0.736344	0.643429
1.000	0.649540	0.250437	0.749750	0.615694
1.250	0.636503	0.227086	0.766732	0.578274
1.500	0.624653	0.204451	0.783124	0.539528
1.750	0.613923	0.183196	0.798464	0.500740
2.000	0.604420	0.163612	0.812567	0.462762
2.500	0.588705	0.129677	0.837028	0.391255
3.000	0.576536	0.102248	0.854994	0.327356
3.500	0.567007	0.080370	0.873269	0.271701
4.000	0.559429	0.063047	0.886609	0.224070
4.500	0.553305	0.049390	0.897638	0.183823
5.000	0.548277	0.038653	0.906848	0.150148
6.000	0.540553	0.023625	0.921237	0.099119
7.000	0.534928	0.014413	0.931716	0.064709
8.000	0.530662	0.008782	0.940018	0.041883
9.000	0.527321	0.005346	0.946433	0.026924
10.000	0.524634	0.003253	0.951614	0.017212
12.500	0.515770	4.3738E-04	0.961038	5.5206E-03
15.000	0.5116509	2.6968E-04	0.967391	1.7365E-03
17.500	0.5116171	7.7502E-05	0.971962	5.3871E-04
20.000	0.512413	2.2258E-05	0.975410	1.6541E-04
25.000	0.509944	1.8334E-06	0.980263	1.5251E-05
30.000	0.508295	1.5085E-07	0.983516	1.3770E-06
35.000	0.507114	1.2403E-08	0.985849	1.2253E-07
40.000	0.506228		0.987603	
60.000	0.504155		0.991712	
80.000	0.503117		0.993776	
100.000	0.502494		0.995017	
125.000	0.501995		0.996011	
150.000	0.501662		0.996674	
175.000	0.501424		0.997148	
200.000	0.501246		0.997504	
250.000	0.500997		0.998003	
300.000	0.500830		0.998335	
400.000	0.500623		0.998751	
500.000	0.500498		0.999001	
600.000	0.500415		0.999167	
800.000	0.500311		0.999375	
1000.000	0.500249		0.999500	
1500.000	0.500166		0.999667	
2000.000	0.500124		0.999750	
3000.000	0.500083		0.999833	
4000.000	0.500062		0.999875	
5000.000	0.500050		0.999900	
8000.000	0.500031		0.999937	
10000.000	0.500025		0.999950	

**Fig. 2** Emissive power at the upper wall for the semi-infinite step case.

$$F_\beta(\tau_0; \tau_0) = 2\mathcal{E}_3(\tau_0, \beta) + \bar{Q}(\tau_0, I + \Delta; \tau_0) + \int_0^I \psi_I(x, \beta) [\bar{Q}_\beta(\tau_0, x; \tau_0) - \bar{Q}_\beta(\tau_0, I + \Delta; \tau_0)] dx \quad (50)$$

where

$$\sqrt{I + \beta^2} \bar{Q}_\beta(0, \mu; \tau_0) / \mu = [I + \beta^2 - \sqrt{I + \beta^2}] R_\beta(\mu, I) / \beta^2 + \int_0^I x' \psi_I(x', \beta) [R_\beta(\mu, x') - R_\beta(\mu, I)] dx' \quad (51)$$

$$\sqrt{I + \beta^2} \bar{Q}_\beta(\tau_0, \mu; \tau_0) / \mu = [I + \beta^2 - \sqrt{I + \beta^2}] T_\beta(\mu, I) / \beta^2 + \int_0^I x' \psi_I(x', \beta) [T_\beta(\mu, x') - T_\beta(\mu, I)] dx' \quad (52)$$

In obtaining these equations, the following two identities were utilized:

$$\int_0^I \psi_I(x, \beta) dx = I \quad \text{and} \quad \int_0^I x \psi_I(x, \beta) dx = [I + \beta^2 - \sqrt{I + \beta^2}] / \beta^2 \quad (53)$$

The quantity Δ was set equal to 10^{-7} in order to avoid the numerical singularity in $T_\beta(1, 1)$. The calculation of the generalized X and Y functions at $\mu = 1$ and $\mu = 1 + \Delta$ brings the total number of differential equations to $2(\bar{N} + \bar{M}) + 4 = 122$.

The preceding system of equations is solved for 64 values of β over a range of τ_0 from zero to ten, and a small portion of the results are tabulated in Tables 2-7. These are the same 64 β

Table 4 Cosine varying results for $\tau_0 = 1.0$

β	$\phi_\beta(0; \tau_0)$	$\phi_\beta(\tau_0; \tau_0)$	$F_\beta(0; \tau_0)$	$F_\beta(\tau_0; \tau_0)$
0.0	0.758146	0.241854	0.553406	0.553406
0.001	0.758146	0.241853	0.553406	0.553406
0.002	0.758146	0.241853	0.553407	0.553405
0.004	0.758144	0.241851	0.553409	0.553402
0.008	0.758139	0.241844	0.553418	0.553393
0.010	0.758133	0.241838	0.553425	0.553380
0.020	0.758095	0.241791	0.553484	0.553301
0.030	0.758030	0.241713	0.553581	0.553171
0.040	0.757939	0.241604	0.553717	0.552988
0.050	0.757822	0.241464	0.553891	0.552753
0.060	0.757680	0.241293	0.554104	0.552466
0.080	0.757319	0.240858	0.554645	0.551738
0.100	0.756857	0.240302	0.555337	0.550805
0.200	0.753098	0.235768	0.560982	0.543174
0.300	0.747167	0.228589	0.569926	0.530900
0.400	0.739492	0.219251	0.581572	0.514951
0.500	0.729566	0.209312	0.595236	0.495867
0.600	0.720288	0.196318	0.610248	0.474555
0.800	0.700547	0.171035	0.642029	0.428152
1.000	0.680938	0.146262	0.673432	0.380440
1.250	0.659901	0.118274	0.704627	0.321298
1.500	0.643415	0.094537	0.740596	0.271502
1.750	0.629753	0.075929	0.767179	0.226051
2.000	0.617131	0.059275	0.789726	0.186972
2.500	0.592495	0.036695	0.824799	0.126016
3.000	0.578423	0.022574	0.850421	0.083659
3.500	0.567962	0.013937	0.869711	0.054931
4.000	0.559920	0.008463	0.884668	0.035746
4.500	0.553560	0.005167	0.896571	0.023096
5.000	0.548411	0.003152	0.906256	0.014835
6.000	0.540592	0.001697E-03	0.921052	6.0350E-03
7.000	0.534940	4.3320E-04	0.931817	2.4195E-03
8.000	0.530466	1.6020E-04	0.939998	9.5965E-04
9.000	0.527332	5.9186E-05	0.946427	3.7733E-04
10.000	0.524634	2.1360E-05	0.951612	1.4735E-04
12.500	0.513770	1.2054E-06	0.961038	1.3726E-05
15.000	0.516509	1.4888E-07	0.967391	1.2493E-06
17.500	0.514171	1.2263E-08	0.971962	1.1188E-07
20.000	0.512413		0.975410	
25.000	0.509944		0.980263	
30.000	0.509295		0.983516	
35.000	0.507114		0.985849	
40.000	0.506228		0.987603	
60.000	0.504155		0.991712	
80.000	0.503117		0.993776	
100.000	0.502494		0.995017	
125.000	0.501695		0.996011	
150.000	0.501662		0.996674	
175.000	0.501424		0.997148	
200.000	0.501246		0.997504	
250.000	0.500997		0.998003	
300.000	0.500830		0.998335	
400.000	0.500623		0.998751	
500.000	0.500498		0.999001	
600.000	0.500415		0.999167	
800.000	0.500311		0.999375	
1000.000	0.500249		0.999500	
1500.000	0.500166		0.999667	
2000.000	0.500124		0.999750	
3000.000	0.500083		0.999833	
4000.000	0.500062		0.999875	
5000.000	0.500050		0.999900	
8000.000	0.500031		0.999937	
10000.000	0.500025		0.999950	

Table 5 Cosine varying results for $\tau_0 = 5.0$

β	$\phi_\beta(0; \tau_0)$	$\phi_\beta(\tau_0; \tau_0)$	$F_\beta(0; \tau_0)$	$F_\beta(\tau_0; \tau_0)$
0.0	0.910079	0.089921	0.207657	0.207657
0.001	0.910078	0.089921	0.207659	0.207656
0.002	0.910075	0.089919	0.207664	0.207652
0.004	0.910065	0.089912	0.207686	0.207636
0.008	0.910024	0.089893	0.207770	0.207573
0.010	0.909994	0.089862	0.207834	0.207526
0.020	0.909739	0.089685	0.208363	0.207132
0.030	0.909316	0.089390	0.209242	0.206677
0.040	0.908725	0.088990	0.210468	0.206157
0.050	0.907971	0.088457	0.212034	0.205404
0.060	0.907056	0.087824	0.213934	0.204997
0.080	0.904758	0.086241	0.218701	0.203978
0.100	0.901870	0.084266	0.224689	0.203085
0.200	0.880325	0.070064	0.269204	0.163411
0.300	0.851558	0.052976	0.327334	0.125049
0.400	0.822343	0.037423	0.387331	0.087776
0.500	0.795510	0.025248	0.442964	0.061778
0.600	0.769555	0.016521	0.492148	0.041356
0.800	0.729382	0.006607	0.571761	0.017664
1.000	0.686779	2.6084E-03	0.631609	7.2895E-03
1.250	0.665848	7.8084E-04	0.683355	2.3532E-03
1.500	0.646304	2.7014E-04	0.728894	7.4786E-04
1.750	0.626989	6.7267E-05	0.760896	2.3517E-04
2.000	0.613136	1.9566E-05	0.786235	7.3344E-05
2.500	0.582789	1.6416E-06	0.873727	6.9950E-06
3.000	0.578508	1.3686E-07	0.857083	6.5328E-07
3.500	0.567987	1.1369E-08	0.869602	6.0099E-08
4.000	0.559927	9.4206E-10	0.884632	5.4394E-09
4.500	0.553563	7.7931E-11	0.896559	4.8772E-10
5.000	0.548412	6.4386E-12	0.906253	4.3342E-11
6.000	0.540592	4.3832E-14	0.921052	3.3508E-13
7.000	0.534940		0.931816	2.5349E-15
8.000	0.530466		0.939998	
9.000	0.527332		0.946427	
10.000	0.524634		0.951612	
12.500	0.513770		0.961038	
15.000	0.516509		0.967391	
17.500	0.514171		0.971962	
20.000	0.512413		0.975410	
25.000	0.509944		0.980263	
30.000	0.509295		0.983516	
35.000	0.507114		0.985849	
40.000	0.506228		0.987603	
60.000	0.504155		0.991712	
80.000	0.503117		0.993776	
100.000	0.502494		0.995017	
125.000	0.501695		0.996011	
150.000	0.501662		0.996674	
175.000	0.501424		0.997148	
200.000	0.501246		0.997504	
250.000	0.500997		0.998003	
300.000	0.500830		0.998335	
400.000	0.500623		0.998751	
500.000	0.500498		0.999001	
600.000	0.500415		0.999167	
800.000	0.500311		0.999375	
1000.000	0.500249		0.999500	
1500.000	0.500166		0.999667	
2000.000	0.500124		0.999750	
3000.000	0.500083		0.999833	
4000.000	0.500062		0.999875	
5000.000	0.500050		0.999900	
8000.000	0.500031		0.999937	
10000.000	0.500025		0.999950	

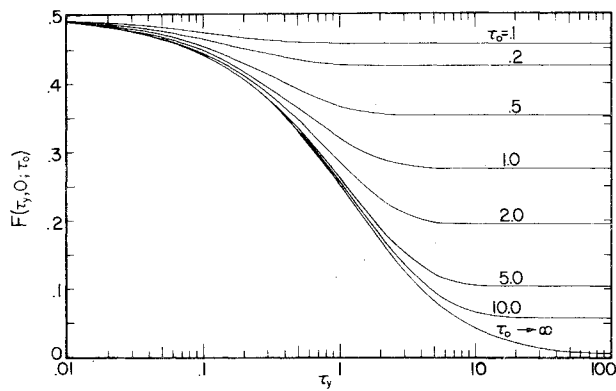


Fig. 3 Radiative flux at the upper wall for the semi-infinite step case.

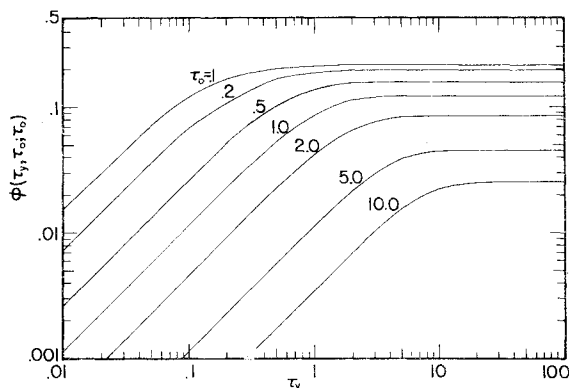


Fig. 4 Emissive power at the lower wall for the semi-infinite step case.

values used by Breig and Crosbie⁷ in their study of a semi-infinite medium. In order to save computer time, the functions ϕ_β and F_β are not calculated at every step, but only at selected values of τ_0 . For $\beta > 8$, to continue the integration to $\tau_0 = 10$ is monetarily prohibitive because the step size is so small. As the optical thickness increases, ϕ_β and F_β at the upper boundary approach constant values, while these functions at the lower boundary approach zero. Thus, when ϕ_β and F_β at the upper boundary converge to eight digits, the program is terminated. Roughly this occurs when $\beta\tau_0 = 20$.

The calculation of ϕ and F can be expressed as¹⁰

$$G(\tau_y) = \frac{1}{\pi} \int_0^\infty g(\beta) \sin(\beta\tau_y) \frac{d\beta}{\beta} = \frac{1}{\pi} \int_0^\infty g(x/\tau_y) \sin x \frac{dx}{x} \quad (54)$$

where $g(\beta)$ is ϕ_β or F_β and G is the corresponding function ϕ and F . The latter integral can be written as an alternating series, i.e.,

$$G(\tau_y) = \frac{1}{2} g(\infty) + \sum_{k=0}^{\infty} (-1)^k S_k(\tau_y) \quad (55)$$

where

$$S_k(\tau_y) = \frac{1}{\pi} \int_0^\pi f[(x+k\pi)/\tau_y] \frac{\sin x dx}{(x+k\pi)} \quad (56)$$

and $f(\beta) = g(\beta) - g(\infty)$. Since $f(\beta)$ approaches zero at large β , the series will converge faster than if just $g(\beta)$ was used. The first term in Eq. (55) represents the small τ_y solution, i.e., $\phi(0, 0; \tau_0) = 1/4$. These integrals, Eqs. (56), must be evaluated numerically; therefore, a procedure for calculating $f(\beta)$ at the

Table 6 Cosine varying results for $\tau_0 = 10.0$

β	$\phi_\beta(0;\tau_0)$	$\phi_\beta(\tau_0;\tau_0)$	$F_\beta(0;\tau_0)$	$F_\beta(\tau_0;\tau_0)$
0.0	0.949448	0.050552	0.116745	0.116745
0.001	0.949446	0.050551	0.116749	0.116743
0.002	0.949441	0.050548	0.116761	0.116735
0.004	0.949419	0.050535	0.116808	0.116705
0.008	0.949333	0.050483	0.115997	0.116587
0.010	0.949268	0.050444	0.117139	0.116498
0.020	0.948730	0.050121	0.118314	0.115760
0.030	0.947842	0.049588	0.120257	0.114545
0.040	0.946612	0.048857	0.122943	0.112875
0.050	0.945057	0.047938	0.126340	0.110778
0.060	0.943193	0.046848	0.130409	0.108289
0.080	0.938624	0.044225	0.140372	0.102298
0.100	0.933086	0.041144	0.152424	0.095258
0.200	0.897301	0.024042	0.229612	0.056079
0.300	0.859336	0.011579	0.309920	0.027336
0.400	0.825191	0.005034	0.380468	0.012080
0.500	0.795543	2.0686E-03	0.440436	5.0647E-03
0.600	0.766917	8.2192E-04	0.491241	2.0592E-03
0.800	0.728425	1.2260E-04	0.571649	3.2399E-04
1.000	0.696784	1.7564E-05	0.631595	4.9258E-05
1.250	0.661889	1.5060E-06	0.681154	4.5677E-06
1.500	0.644394	1.2714E-07	0.728898	4.1734E-07
1.750	0.626989	1.0645E-08	0.763896	3.7756E-08
2.000	0.613186	8.8697E-10	0.786235	3.3899E-09
2.500	0.592789	6.1077E-12	0.823727	2.6807E-11
3.000	0.576808	4.1797E-14	0.850883	2.0768E-13
3.500	0.567287	2.8490E-16	0.869602	1.5822E-15
4.000	0.559277	1.9386E-18	0.884632	1.1488E-17
4.500	0.553563	1.3165E-20	0.896559	8.3039E-20
5.000	0.548412	9.9290E-23	0.906253	6.4974E-22
6.000	0.540592	4.0963E-27	0.921052	3.4377E-26
7.000	0.534840	1.8746E-31	0.931816	1.7756E-30
8.000	0.530666		0.939988	
9.000	0.527322		0.946427	
10.000	0.524634		0.951612	
12.500	0.519770		0.961038	
15.000	0.516509		0.967391	
17.500	0.514171		0.971962	
20.000	0.512413		0.975410	
25.000	0.509944		0.980263	
30.000	0.508295		0.983516	
35.000	0.507114		0.985849	
40.000	0.506228		0.987603	
60.000	0.504155		0.991712	
80.000	0.503117		0.993776	
100.000	0.502494		0.995017	
125.000	0.501995		0.996011	
150.000	0.501662		0.996674	
175.000	0.501424		0.997148	
200.000	0.501246		0.997504	
250.000	0.500597		0.998003	
300.000	0.500830		0.998335	
400.000	0.500623		0.998751	
500.000	0.500498		0.999001	
600.000	0.500415		0.999167	
800.000	0.500311		0.999375	
1000.000	0.500249		0.999500	
1500.000	0.500166		0.999667	
2000.000	0.500124		0.999750	
3000.000	0.500083		0.999833	
4000.000	0.500062		0.999875	
5000.000	0.500050		0.999900	
8000.000	0.500031		0.999937	
10000.000	0.500025		0.999950	

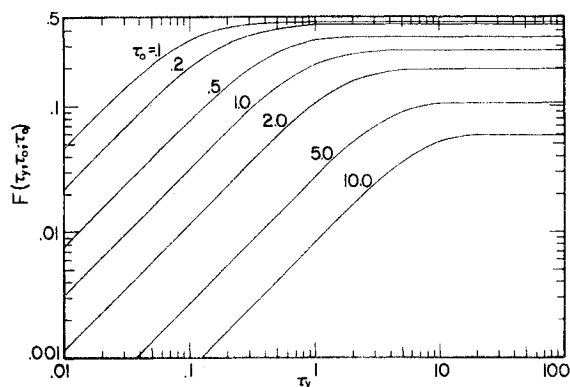


Fig. 5 Radiative flux at the lower wall for the semi-infinite step case.

quadrature points is necessary. Based on monetary considerations, $f(\beta)$ at these points cannot be calculated directly; thus a fourth-order Aikens interpolation technique and the results of the 64 β values are utilized. For accurate interpolation between so few points, very accurate values of $f(\beta)$ at the 64 β values are necessary. When the series is slowly convergent ($\tau_y > 1$), accurate values of S_k are necessary to obtain moderately accurate values of G . In other words, there can be large losses in accuracy in evaluating the series. The natural logarithm of $|f(\beta)|$ is taken for interpolation because oscillations occur when $f(\beta)$ is interpolation at large β .

The first fifteen integrals are calculated using a fifteenth-order Gaussian quadrature. The first integral is divided and recalculated and checked against the undivided result. When these two results do not agree to five decimal places, the integral is subdivided until this error criteria is met. The

Table 7 Emissive power and radiative flux at the boundaries for the semi-infinite step case

τ_y	$\phi(\tau_y, 0; \tau_0)$	$\phi(\tau_y, \tau_0; \tau_0)$	$F(\tau_y, 0; \tau_0)$	$F(\tau_y, \tau_0; \tau_0)$
$\tau_0 = 0.1$				
0.0	0.25000	0.0	0.50000	0.0
0.01	0.25345	0.15217D - 01	0.49382	0.46814D - 01
0.02	0.25580	0.30130D - 01	0.48983	0.92241D - 01
0.05	0.26088	0.70645D - 01	0.48174	0.20998D 00
0.10	0.26641	0.11909D 00	0.47390	0.33063D 00
0.20	0.27281	0.16608D 00	0.46641	0.41533D 00
0.50	0.28029	0.20125D 00	0.46028	0.45167D 00
1.00	0.28373	0.21107D 00	0.45848	0.45678D 00
2.00	0.28518	0.21398D 00	0.45794	0.45773D 00
5.00	0.28550	0.21448D 00	0.45785	0.45785D 00
10.00	0.28551	0.21449D 00	0.45785	0.45785D 00
100.00	0.28551	0.21449D 00	0.45785	0.45785D 00
$\tau_0 = 0.5$				
0.0	0.25000	0.0	0.50000	0.0
0.01	0.25431	0.26565D - 02	0.49183	0.76746D - 02
0.02	0.25753	0.53106D - 02	0.48585	0.15339D - 01
0.05	0.26519	0.13235D - 01	0.47186	0.38177D - 01
0.10	0.27492	0.26181D - 01	0.45453	0.75168D - 01
0.20	0.28904	0.50239D - 01	0.43025	0.14181D 00
0.50	0.31335	0.10122D 00	0.39135	0.26538D 00
1.00	0.33074	0.13624D 00	0.36686	0.32806D 00
2.00	0.34078	0.15255D 00	0.35493	0.34852D 00
5.00	0.34361	0.15627D 00	0.35213	0.35303D 00
10.00	0.34367	0.15633D 00	0.35208	0.35208D 00
100.00	0.34367	0.15633D 00	0.35208	0.35208D 00
$\tau_0 = 1.0$				
0.0	0.25000	0.0	0.50000	0.0
0.01	0.25455	0.11524D - 02	0.49124	0.31441D - 02
0.02	0.25802	0.23045D - 02	0.48468	0.62872D - 02
0.05	0.26642	0.57564D - 02	0.46894	0.15700D - 01
0.10	0.27736	0.11478D - 01	0.44871	0.31270D - 01
0.20	0.29389	0.22683D - 01	0.41869	0.61537D - 01
0.50	0.32499	0.52544D - 01	0.36387	0.13900D 00
1.00	0.35140	0.85707D - 01	0.31936	0.21502D 00
2.00	0.37103	0.11144D 00	0.28830	0.26269D 00
5.00	0.37882	0.12065D 00	0.27704	0.27635D 00
10.00	0.37907	0.12093D 00	0.27670	0.27670D 00
100.00	0.37907	0.12093D 00	0.27670	0.27670D 00
$\tau_0 = 5.0$				
0.0	0.25000	0.0	0.50000	0.0
0.01	0.25481	0.11451D - 03	0.49064	0.27262D - 03
0.02	0.25853	0.22902D - 03	0.48347	0.54525D - 03
0.05	0.26769	0.57251D - 03	0.46591	0.13631D - 02
0.10	0.27991	0.11448D - 02	0.44264	0.27256D - 02
0.20	0.29898	0.22881D - 02	0.40658	0.54472D - 02
0.50	0.33758	0.56932D - 02	0.33395	0.13548D - 01
1.00	0.37569	0.11199D - 01	0.26187	0.26612D - 01
2.00	0.41419	0.21039D - 01	0.18744	0.49759D - 01
5.00	0.44728	0.38181D - 01	0.12036	0.88934D - 01
10.00	0.45440	0.44326D - 01	0.10522	0.10245D 00
20.00	0.45503	0.44955D - 01	0.10384	0.10382D 00
50.00	0.45504	0.44961D - 01	0.10383	0.10383D 00
100.00	0.45504	0.44961D - 01	0.10383	0.10383D 00
$\tau_0 = 10.0$				
0.0	0.25000	0.0	0.50000	0.0
0.01	0.25484	0.35169D - 04	0.49058	0.82000D - 04
0.02	0.25858	0.70338D - 04	0.48335	0.16400D - 03
0.05	0.26782	0.17584D - 03	0.46561	0.40999D - 03
0.10	0.28016	0.35167D - 03	0.44205	0.81994D - 03
0.20	0.29948	0.70319D - 03	0.40540	0.16396D - 02
0.50	0.33884	0.17555D - 02	0.33101	0.40929D - 02
1.00	0.37821	0.34939D - 02	0.25601	0.81449D - 02
2.00	0.41916	0.68554D - 02	0.17589	0.15973D - 01
5.00	0.45847	0.15186D - 01	0.09437	0.35286D - 01
10.00	0.47136	0.22293D - 01	0.06597	0.51593D - 01
20.00	0.47452	0.25074D - 01	0.05883	0.57915D - 01
50.00	0.47473	0.25277D - 01	0.05837	0.58374D - 01
100.00	0.47472	0.25276D - 01	0.05837	0.58372D - 01

second integral is evaluated in the same manner. The remaining integrals are calculated without subdivision. These fifteen integrals are then fed into Euler transform subprogram to speed convergence. A short listing of these results is found in Table 7.

Results and Discussion

The emissive power and radiative flux at the boundaries for the cosine-varying case are presented in Tables 2-6 for five optical thicknesses. These represent less than 1% of the results obtained. The β results are quite important because solutions for almost any spatial variation of incident radiation can be

calculated from them. The emissive powers at the boundaries and the radiative fluxes leaving the medium decrease as the spatial frequency increases. Note that the radiative flux leaving the upper boundary is $1 - F_\beta(0; \tau_0)$. This behavior is simply explained by the fact that the amount of radiant energy per unit time, per unit length incident on the medium in a strip $(-\tau_b \leq \tau_y \leq \tau_b)$ is $2\sin(\beta\tau_b)/\beta$ and decreases with β . For $\tau_0 \geq 0.1$, the largest difference between the finite and semi-infinite results is $2.3(10)^{-5}$ for $\beta\tau_0 \geq 10$, while the largest difference between the two-dimensional and one-dimensional ($\beta = 0$) results is $2.0(10)^{-4}$ for $\beta\tau_0 \leq 0.01$.

Figures 2 and 3 illustrate the variation of emissive power and flux across the upper boundary for the semi-infinite step case, while the results at the lower boundary are given in Figs. 4 and 5. The emissive powers at the boundaries and the radiative flux leaving the medium increase with optical distance away from the origin. Note that the radiative flux leaving the upper boundary is $1 - F(\tau_y, 0; \tau_0)$. Near the origin, the medium "sees" the low temperature wall on the other side. Moving away from the origin, the medium itself acts as a shield and reduces the influence of the temperature jump. At large optical distances away from the origin, the medium cannot "see" the temperature jump and the problem is one-dimensional. The distance from the origin at which the one-dimensional approximation is valid depends on the optical thickness of the medium. As a conservative approximation, the one-dimensional analysis can be applied when $\tau_y \geq 1.5 + 2\tau_0$. The maximum percentage error of this approximation is 1%. When the optical thickness of the medium is large, the finite medium can be approximated by a semi-infinite medium. The maximum difference between the semi-infinite and finite medium occurs for the one-dimensional case ($\tau_y \rightarrow \infty$). For $\tau_0 = 10$, the difference is 0.025 for the emissive power and 0.058 for the radiative flux. If τ_y is set equal to $1/\beta$, the semi-infinite step results follow the behavior of the cosine-varying results.

All these results can simply be extended to a nongray medium with spectral windows.¹⁵ If both the absorption and scattering coefficients have the same spectral shape, i.e., $\kappa_\nu = \kappa\alpha(\nu)$ and $\sigma_{s\nu} = \sigma_s\alpha(\nu)$, and the function $\alpha(\nu)$ is allowed only two values—zero or unity. The bands or continuum are approximated by rectangular boxes of equal height; however, the number, location, and width of the bands are unrestricted. The energy equation reduces to a form identical to the gray case, whereas the expression radiative flux includes an additional term to account for the radiant interchange through the spectral windows.

Conclusions

When the wall temperature distributions can be represented by a series of steps, the emissive power and radiative flux can be expressed in terms of those for the semi-infinite step case. This fact greatly reduces the number of calculations. Discontinuities in the wall temperatures produce discontinuities in the emissive power and radiative flux. Results for the emissive power and radiative flux at the walls can be obtained without calculating the internal values. For other

wall temperature distributions, the emissive power and radiative flux can be calculated from the cosine-varying results.

Acknowledgment

This work was supported in part by the National Science Foundation through Grants NSF ENG 72 04103 and NSF ENG 74 22107.

References

- ¹Crosbie, A. L. and Linsenbardt, T. L., "Two-Dimensional Isotropic Scattering in a Semi-Infinite Medium," *Journal of Quantitative Spectroscopy and Radiative Transfer*, Vol. 19, 1978, pp. 257-284.
- ²Bobco, R. P., "Directional Emissivities From a Two-Dimensional, Absorbing-Scattering Medium; the Semi-Infinite Slab," *Journal of Heat and Transfer*, Vol. C89, 1967, pp. 313-320.
- ³Love, T. J. and Turner, W. D., "Directional Emittance from an Emitting, Absorbing, and Scattering Media," *Progress in Astronautics and Aeronautics, Thermophysics: Applications to Thermal Design of Spacecraft*, edited by J. T. Bevens, Vol. 23, AIAA, New York, 1970, pp. 319-327.
- ⁴Turner, W. D. and Love, T. J., "Directional Emittance of a Two-Dimensional Ceramic Coating," *AIAA Journal*, Vol. 9, Sept. 1971, pp. 1849-1853.
- ⁵Stockham, L. W. and Love, T. J., "Radiative Heat Transfer from a Cylindrical Cloud of Particles," *AIAA Journal*, Vol. 6, Oct. 1968, pp. 1935-1940.
- ⁶Breig, W. F. and Crosbie, A. L., "Two-Dimensional Radiative Equilibrium," *Journal of Mathematical Analysis and Applications*, Vol. 46, April 1974, pp. 104-125.
- ⁷Breig, W. F. and Crosbie, A. L., "Two-Dimensional Radiative Equilibrium: A Semi-Infinite Medium Subjected to Cosine Varying Radiation," *Journal of Quantitative Spectroscopy and Radiative Transfer*, Vol. 13, 1973, pp. 1395-1419.
- ⁸Breig, W. F. and Crosbie, A. L., "Two-Dimensional Radiative Equilibrium: A Semi-Infinite Medium Subjected to a Finite Strip of Radiation," *Journal of Quantitative Spectroscopy and Radiative Transfer*, Vol. 14, 1974, pp. 189-209.
- ⁹Breig, W. F. and Crosbie, A. L., "Two-Dimensional Radiative Equilibrium: Boundary Emissive Powers for a Finite Medium Subjected to Cosine Varying Radiation," *Journal of Quantitative Spectroscopy and Radiative Transfer*, Vol. 14, 1974, pp. 1209-1237.
- ¹⁰Breig, W. F. and Crosbie, A. L., "Two-Dimensional Radiative Equilibrium: Boundary Fluxes for a Finite Medium Subjected to Cosine Varying Radiation," *Journal of Quantitative Spectroscopy and Radiative Transfer*, Vol. 15, 1975, pp. 163-179.
- ¹¹Joseph, J. H., Wiscombe, W. J., and Weinman, J. A., "The Delta-Eddington Approximation for Radiative Flux Transfer," *Journal of Atmospheric Sciences*, Vol. 33, Dec. 1976, pp. 2452-2459.
- ¹²Breig, W. F. and Crosbie, A. L., "Numerical Computation of a Generalized Exponential Integral Function," *Mathematics of Computation*, Vol. 28, No. 126, 1974, pp. 575-579.
- ¹³Taitel, Y., "Formulation of Two-Dimensional Radiant Heat Flux for Absorbing-Emitting Plane with Nonisothermal Bounding Walls," *AIAA Journal*, Vol. 7, Oct. 1969, pp. 1832-1837.
- ¹⁴Froberg, C. E., *Introduction to Numerical Analysis*, Addison-Wesley Publishing Co., Reading, Mass., 1969, p. 172.
- ¹⁵Crosbie, A. L., "Two-Dimensional Radiative Equilibrium: A Simple Nongray Problem," *AIAA Journal*, Vol. 14, Nov. 1976, pp. 1649-1652.